ALAN F. BEARDON, TOMASZ DUBEJKO* AND KENNETH STEPHENSON*

SPIRAL HEXAGONAL CIRCLE PACKINGS IN THE PLANE

ABSTRACT. We discuss an intriguing geometric algorithm which generates infinite spiral patterns of packed circles in the plane. Using Kleinian group and covering theory, we construct a complex parametrization of all such patterns and characterize those whose circles have mutually disjoint interiors. We prove that these 'coherent' spirals, along with the regular hexagonal packing, give all possible hexagonal circle packings in the plane. Several examples are illustrated.

1. INTRODUCTION

This paper concerns patterns of circles in the plane which we will call hexagonal circle packings. Their basic unit is the *flower*, consisting of a *center* circle tangent to and surrounded by *petals*. A *hexagonal* flower is illustrated in Figure 2(i); the six petals form a closed chain (each tangent to the next, the last tangent to the first) which wraps once in the positive direction about the center. A hexagonal circle packing is a collection P of circles wherein each circle is the center of a hexagonal flower. Most familiar is the *regular hexagonal packing* in which all the circles have the same radius (the 'penny' packing). However, this is an example of a 'coherent' packing, meaning one in which the circles have mutually disjoint interiors; the generic case we will encounter is more general, involving overlapping circles and even extraneous tangencies–we give a precise definition of 'circle packing' shortly.

The issue of the paper is whether there exist hexagonal circle packings other than the regular ones. It happens that there is an elegant little geometric algorithm for generating spiral patterns which, to the authors' knowledge, provides the only additional hexagonal circle packings. Figure 1 is a computer-generated example of one of these spirals, and it would appear to be coherent. This paper was motivated by the desire to understand how and why the geometric algorithm works and to determine whether it can in fact generate coherent packings (i.e. are the computer pictures accurate?).

As it turns out, analysis of the algorithm leads us to a family of spiral packings parametrized by a complex variable (Theorem 4), and among these we find a countably infinite family of coherent ones. Moreover, we show

*The last two authors gratefully acknowledge support of the National Science Foundation and the Tennessee Science Alliance.

Geometriae Dedicata **49**: 39–70, 1994.

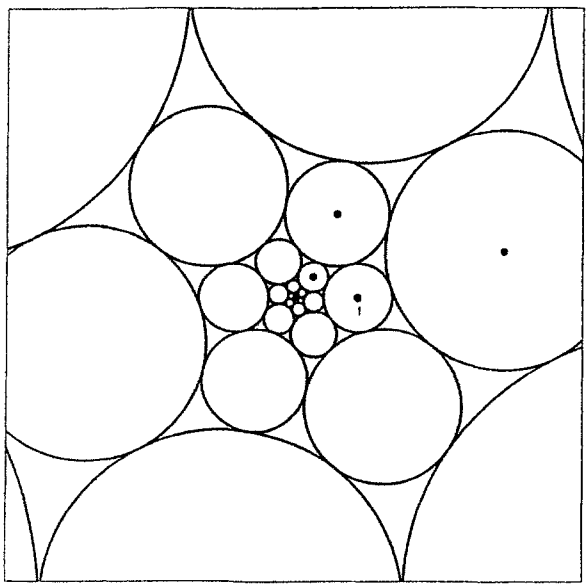

Fig. 1. A coherent spiral circle packing?

(Theorem 7) that the latter, along with the regular hexagonal packing, comprise all possible coherent hexagonal circle packings in the plane (up to similarity). Whether there exist additional non-coherent hexagonal packings remains an open question.

Though the circle configurations of this paper will be generated by a specific algorithm, we provide this general definition of circle packing:

A collection P of circles in the plane is a '*circle packing*' if P is a union of flowers satisfying the following conditions:

(1) Every circle is the center of a designated flower.
(2) Whenever B_1, B_2, B_3 are successive petals of the flower with center C, then B_3, C, B_1 must be successive petals of the flower with center B_2.
(3) Any two circles can be connected by a finite chain of circles in which each is a petal of its pedecessor.

If any two circles of P are identical or have mutually disjoint interiors, then P is termed '*coherent*'. We say that P is '*hexagonal*' if all its flowers are hexagonal.

We should point out that in parts of the literature, the term 'packing' would imply mutually disjoint interiors, making our term 'coherent' redundant. However, circle packings provide a genralization of the coherent ones much

as multi-sheeted covering surfaces generalize plane domains. This is a valuable analogy, since our spirals may be pictured as lying on infinite-sheeted coverings of the punctured plane—only in countably many cases do the circles of different sheets line up, so that the pattern projects to a coherent circle packing in the plane. We also note that there is a rapidly growing body of work regarding circle packings, often with connections to classical analytic functions. In this vein, the spiral circle packings of this paper should be seen as analogues of exponential functions. (See [RS] and [BSt].) Circle packings have provided an important means for constructing hyperbolic 3-manifolds (see [T, Ch. 13]), and our parametrized family of packings may be useful in this regard. For connections with phyllotaxis, see Section 7(e).

Let us begin where the authors began, namely with a fascinating observation of Peter Doyle: Let C_0 be the unit circle in the complex plane $\mathbf{C}$. Given positive numbers a and b, one can construct six circles $C_1, C_2, \ldots, C_6$ of radii $a, b, b/a$, $1/a$, $1/b$, and a/b, respectively, such that all are tangent to C_0, each C_j is tangent to $C_{j+1}, j = 1, \ldots, 5$, and the last, C_6, is tangent to the first, C_1: this is illustrated in Figure 2(i) with $a = 3/2$ and $b = 3/4$. We leave the reader to verify the surprising fact that the configuration fits together as described, forming a hexagonal flower. (Note that more extreme values of a and b will yield hexagonal flowers having (non-contiguous) petals which overlap; that is perfectly acceptable.)

Of course, taking C_0 to be the unit circle is simply a normalization: the general rule is that given three mutually tangent (and exterior) circles C_0, C_1, and C_2, with radii R_0, R_1, and R_2, respectively, we construct a fourth circle C_3 of radius R_3, located as illustrated in Figure 2(ii), where R_3 is given by

$$R_0R_2 = R_1R_3 \tag{1}$$

We then use C_0, C_2, C_3 to construct C_4 and so on, and as $C_7 = C_1$, this produces a flower with center C_0.

An ordered triple (C_0, C_1, C_2) of circles, mutually tangent and exterior to each other, will be called a *cell*. Starting with a fixed cell, our *algorithm* consists of adjoining an additional circle to the cell (C_0, C_1, C_2) to get a quadrilateral as in Figure 2(ii), R_3 being determined by (1). We call this *cell continuation* and the reader may think of it as a process which is analogous to the analytic continuation of some analytic function element.

It is this algorithm which we would like to understand—in particular, what happens when one applies it repeatedly? That is, starting with a given cell, one creates all possible circles by repeated application of the algorithm

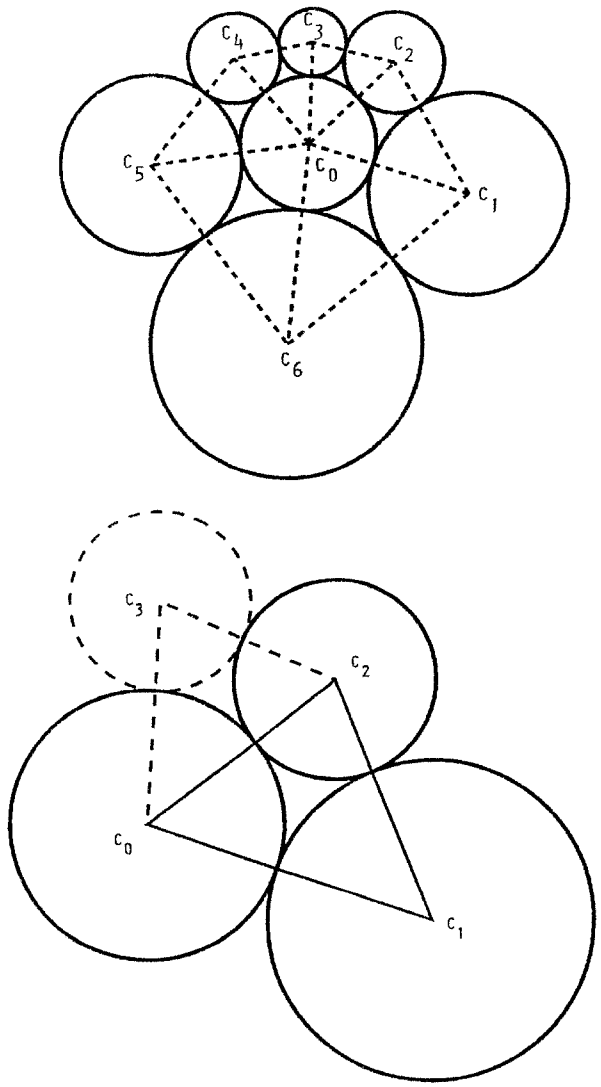

Fig. 2. (i) A flower, (ii) the construction step.

in all directions (analogous to the complete analytic function determined by a given function element). As we shall see, this leads naturally to the construction of a surface (surprisingly, always the smooth covering of a punctured plane) and to an associated discrete group action. Because of the geometry of circles, a very pleasing connection can be established between cells and certain classical curves called 'Ovals of Descartes'. In conjunction

with a tricky little technical lemma, this leads us to a family of exponential mappings parametrized by a complex variable and associated with the various cell continuations. Within this family, each of a certain discrete set of parameters provides a coherent circle packing (loosely analogous to a single-valued analytic function). Putting together some facts from the recent literature, especially a uniqueness result of Oded Schramm, we prove that these special spirals, along with the regular hexagonal packing, comprise all possible coherent hexagonal circle packings in the plane. We close with some additional comments in Section 7.

The figures in the paper were prepared by the third author on a SUN Sparcstation (Table I in Section 7 gives the parameters for all the illustrated spirals). However, the geometric algorithm can be implemented easily on almost any machine, and coherent spirals can be found with a little experimentation. Indeed, our results explain why a whole spiral will automatically become coherent if one can, through *ad hoc* adjustments, force a single pair of circles to share the same center.

2. THE ASSOCIATED MANIFOLD

Given a cell (C_0, C_1, C_2), we can form the non-degenerate triangle T with vertices z_0, z_1, and z_2 and, conversely, any triangle T arises from a unique cell in this way. Consequently, we can consider the algorithm as follows: starting with a triangle T, construct the associated cell (C_0, C_1, C_2) for T; then apply the algorithm to produce C_3, say opposite z_1; and finally, join the centers of C_0, C_2, and C_3 to produce a new traingle T'. With this interpretation, the algorithm attaches to a triangle T a new triangle T' which shares a specified edge with T, and in this way, repeated applications of the algorithm lead automatically to the construction of an abstract triangulated 2-manifold M (whose charts simply locate the triangles in $\mathbf{C}$).

The existence of the original flower implies that as we construct M by joining together triangles around a common vertex z_0, the algorithm repeats the triangles cyclically (with period six) and it is natural to identify these repeated triangles. We do this, and with this convention, M is automatically a smooth (unbranched) manifold.

THEOREM 1. *Suppose that the cell (C_0, C_1, C_2) is generic; that is, not all three radii are the same. Then there is some point $\zeta \in \mathbf{C}$ such that M is a smooth unlimited covering surface of the punctured plane $\mathbf{C}\backslash\{\zeta\}$. Further, all the circles obtained by repeated cell continuation lie in $\mathbf{C}\backslash\{\zeta\}$.*

Proof. Given the cell (C_0, C_1, C_2) we construct C_3 as above; let Q be the

quadrilateral with vertices z_0, z_1, z_2, and z_3 and define Euclidean similarities f and g (of the form $z \mapsto az + b$) by

$$f(z_0) = z_1, \quad f(z_3) = z_2, \quad g(z_0) = z_3, \quad g(z_1) = z_2.$$

The maps f and g are the *side-pairing maps* of Q and they generate a group which we denote by $G(Q)$.

The essence of the proof of Theorem 1 is to show that repeated cell continuation is achieved by the action of the group $G(Q)$ and through this we are able to understand the real significance of the rather curious rule (1).

The algebraic structure of $G(Q)$ is easily found. As f and g are Euclidean similiarities, their commutator $fgf^{-1}g^{-1}$ is a translation (possibly the identity). As the commutator fixes z_2 it must be the identity, so $G(Q)$ is an abelian group on two generators. Now f and g cannot both be of finite order, for then they would be Euclidean rotations (and hence isometries) and Q would have opposite sides of equal length. This would imply that Q is a parallelogram, and hence that f and g were translations (which have infinite order). We deduce that $G(Q)$ is an infinite group and so is isomorphic to one of $\mathbf{Z} \times \mathbf{Z}$, $\mathbf{Z} \times \mathbf{Z}_r$ (where r is a positive integer), or $\mathbf{Z}$. Each of these can occur and we shall see later how these forms relate to spiral packings; for example, only the last two cases can correspond to coherent packings.

We now examine the geometry of the action of $G(Q)$ and there are two cases to consider according to whether Q is a parallelogram or not. In the first case Q is a parallelogram and, by simple geometry, we have $R_0 = R_1 = R_2 = R_3$ and the associated cell continuation leads to the regular hexagonal packing of the plane. Note that in this case, f and g are translations and a necessary and sufficient condition for this to be so is $z_0 + z_2 = z_1 + z_3$. This case is of little interest.

The second case is when Q is not a parallelogram (we say Q is *generic*) and we concentrate our efforts on this case. Since f and g cannot both be translations, one of them, say f, has a unique fixed point ζ in the plane. Because $fg = gf$, we find that g also fixes ζ. A completely elementary calculation shows that

$$\zeta = \frac{z_2 z_0 - z_1 z_3}{(z_0 + z_2) - (z_1 + z_3)}$$

and we note that, as Q is generic, the denominator is non-zero. Now ζ cannot lie on ∂Q, for each point of ∂Q is moved by either f or g. As ζ varies continuously with the points z_j, it is clear that when we continuously deform Q, either ζ remains inside Q or it remains outside Q. When Q is nearly a parallelogram ζ is close to ∞ and from this we deduce that ζ *is always*

outside Q: this is an important observation. To summarize, when Q is generic, $G(Q)$ *is a group of Euclidean similarities acting on the punctured plane* $\mathbf{C}\backslash\{\zeta\}$ *and the quadrilateral* Q *lies in* $\mathbf{C}\backslash\{\zeta\}$. By choosing coordinates appropriately, we may assume that $\zeta = 0$ and $z_0 = 1$. As $\zeta = 0$, f and g take the form $z \mapsto cz$ and as Q is generic, not both f and g are isometries. Writing

$$f(z) = \alpha z, \quad g(z) = \beta z, \tag{2}$$

we may assume that Q has the (positively ordered) vertices $\{z_0, z_1, z_2, z_3\}$ with the following normalization:

$$\zeta = 0,\ z_0 = 1,\ z_1 = \alpha,\ z_2 = \alpha\beta,\ z_3 = \beta,\ |\alpha| \geqslant 1. \tag{3}$$

The punctured plane $\mathbf{C}\backslash\{0\}$ is denoted $\mathbf{C}^*$.

We return now to the rule (1). Given two cells (C_0, C_1, C_2) and (C_0, C_2, C_3), it is easy to see that (1) is equivalent to each of the conditions

(a) $f(C_0) = C_1$ and $f(C_3) = C_2$;

(b) $g(C_0) = C_3$ and $g(C_1) = C_2$;

and with these, we see that we can either construct C_3 by cell continuation, or as the image $g(C_0)$ $(= f^{-1}(C_2))$, and the result is the same This fact shows that repeated cell continuation leads to circles which are the images of the original circles under $G(Q)$ and conversely, and we leave the proof of this to the reader. We have now shown that, with (1), *we can study repeated cell continuation by studying* $G(Q)$.

It is clear that the manifold M obtained by adjoining consecutive triangles in the repeated cell continuation (as described above) is a smooth covering surface of $\mathbf{C}^*$. Moreover, as the original three circles lie in the union of the $G(Q)$-images of Q, the same is true of all of the circles obtained by continuation, hence the last assertion in Theorem 1 is verified.

It remains to show that M is an *unlimited* covering surface of $\mathbf{C}^*$, but this is an immediate consequence of

(a) Q is a compact subset of $\mathbf{C}^*$, and

(b) f and g are isometries of $\mathbf{C}^*$ when it is endowed with the metric ρ arising from $ds = |dz|/z$.

Indeed, there is a positive δ such that any curve in $\mathbf{C}^*$ that starts inside Q has an initial segment which lifts to a curve in M which (when located in $\mathbf{C}^*$) ends at a point at least a distance δ beyond Q. By (b), the same is true for any $G(Q)$-image of Q; hence all curves in $\mathbf{C}^*$ can be lifted to M and the proof of Theorem 1 is complete. □

Note for later that in a cell continuation two circles with the same centers are the same circles. Indeed, we have seen that all circles are images of C_0.

If $f^a g^b(C_0)$ and $f^c g^d(C_0)$ have the same center η, then $f^a g^b(z_0) = \eta = f^c g^d(z_0)$. Assuming (3), this implies that $f^{a-c} g^{b-d}$ fixes 0, η, and ∞. In particular, $f^{a-c} g^{b-d}$ is the identity, so $f^a g^b(C_0) = f^c g^d(C_0)$.

3. THE GEOMETRY OF CIRCLE PACKING QUADRILATERALS

The analysis in the previous proof is largely independent of circles: given a general quadrilateral Q, even non-convex, one gets the side-pairing maps, the common fixed point outside Q, the abelian group of Euclidean similarities, the surface M, and so forth. What distinguishes quadrilaterals associated with circles? Consider a general quadrilateral Q as being formed by adjoining a triangle T with vertices z_0, z_1, z_2 to a triangle T' with vertices z_0, z_2, z_3 along their common edge $[z_0, z_2]$. We ask for conditions which imply that T' arises from T by the process of cell continuation.

THEOREM 2. *Let Q be the quadrilateral formed by T and T', and assume the normalization of* (3). *Then T' arises from T by cell continuation if and only if for some $\lambda > 1$ the points z_1, z_2, z_3 lie on a common λ-level curve of the function*

$$k(z) = \frac{1 + |z|}{|1 - z|}. \tag{4}$$

Proof. The quadrilateral Q is illustrated in Figure 3, with side lengths labeled by a, b, c, d, e. Each triangle is associated with a unique cell whose radii can be determined easily from the side lengths. Let R_0, R_1, R_2 be the radii for T, and R'_0, R'_2, R'_3 the radii for T'. Then, for example, $2R_0 = a + e - b$, and $2R'_0 = e + d - c$.

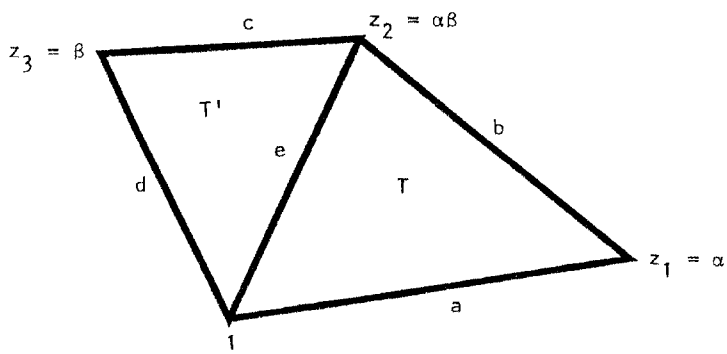

Fig. 3. Triangles forming quadrilateral Q.

The proof is essentially a matter of noting that

$$|\alpha - 1| = a,\ |\beta - 1| = d,\ |\alpha| = \frac{|\alpha\beta - \alpha|}{|\beta - 1|} = \frac{b}{d},\ |\beta| = \frac{c}{a}.$$

With these observations, the condition

$$k(\alpha) = \frac{1 + |\alpha|}{|\alpha - 1|} = \frac{1 + |\beta|}{|\beta - 1|} = k(\beta) \tag{5}$$

is equivalent to $a - b = d - c$, and hence to

$$R_0 = R_0',\ R_2 = R_2'. \tag{6}$$

Explicitly, (5) is the condition for the circles at z_0 and z_2 to be the same for both T and T'.

Suppose now that T' arises from T by cell continuation. Then (5) holds and, in addition,

$$R_0 R_2 = R_1 R_3. \tag{7}$$

Expressing (7) in terms of a, b, c, d, e, we see that it implies that $k(\alpha) = k(\alpha\beta)$; conversely, if $k(\alpha) = k(\beta) = k(\alpha\beta)$, then (6) and (7) hold. This shows that T' arises from T by cell continuation if and only if the points z_1, z_2, z_3 lie on a common level curve of the function k. □

The level curves associated with (4) belong to a family of curves known in classical geometry as 'Ovals of Descartes', which are defined by linear relations in bipolar coordinates. (See [L, p. 188 and Fig. 123].) The heavy curve D is such an oval in Figure 4, which illustrates the theorem. The circle C_0 is centered at $z_0 = 1$, and the vertices z_1, z_2, z_3 of Q are the centers of three petals of the flower with center C_0. We can propagate these in the positive direction about C_0 using the side-pairings and thereby obtain the centers z_4, z_5, z_6 (in positive order) for the remaining three petals. One readily verifies

$$z_j z_{j+3} = 1, \qquad z_j z_{j+2} = z_{j+1}, \quad j = 1, 2, 3.$$

The function k is invariant under $z \mapsto 1/z$, so along with Theorem 2 these relations imply that all six petals of the flower about C_0 are centered on the same oval of Descartes. More is true: since k is invariant under $z \mapsto \bar{z}$, the complex conjugate flower also has its six centers on the same oval. Any cell taken from the flower will generate the same infinite circle packing and every cell from the conjugate flower will generate its conjugate. It is important for the sequel that we use this flexibility to make a normalization in addition

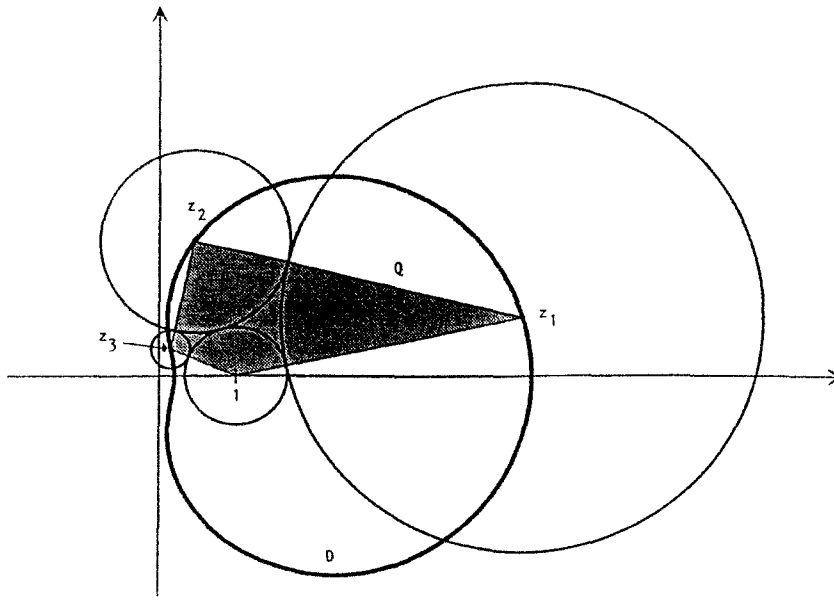

Fig. 4. A quadrilateral and its level curve of k.

to (3): By conjugation and relabeling, if necessary, assume z_1, z_2, z_3 lie in the upper half plane and are centers of successive circles in the flower, in counterclockwise order. Further, by applying the map $z \mapsto 1/\bar{z}$ and relabeling again, if necessary, we arrive at

$$(8) \qquad |z_1| > 1,\ |z_2| \geqslant 1,\ 0 \leqslant \operatorname{Arg}(z_1) \leqslant \operatorname{Arg}(z_3) \leqslant \operatorname{Arg}(z_2) < \pi.$$

In verifying this, it helps to recall that $z_2 = z_1 z_3$ and to note that as a point travels counterclockwise about the part of a level curve of k in the upper half plane its modulus is strictly decreasing. Finally, a moment's reflection will show that there is no other quadrilateral satisfying (3) and (8) which generates the same circle packing. The quadrilateral of Figure 4 is in this normalized position.

We adhere to this normalization to get uniqueness of the packings generated in the next section. The cases of equality regarding arguments in (8) are extreme cases which play a role in later computations: $\operatorname{Arg}(z_1) = \operatorname{Arg}(z_3)$ implies $|z_2| = 1$, whence $|z_1| = |z_3|^{-1}$; here Q is symmetric with respect to the unit circle, with z_2 being the point in the upper half plane where the level curve of k crosses the unit circle. On the other hand, when $\operatorname{Arg}(z_2) = \operatorname{Arg}(z_3)$, then these two arguments are positive, $z_2 = 1/\bar{z}_3$, and z_1 is real.

4. PARAMETRIZING CELL CONTINUATIONS

We now have the tools needed to provide a practical parametrization of the circle configurations obtained by cell continuation. The proof will reduce to the very technical Lemma 3. However, the motivation is a simple analogy between spiral circle packings and the classical exponential mapping $z \mapsto e^z$.

The exponential map is simply periodic and maps the plane $\mathbf{C}$ onto the punctured plane $\mathbf{C}^*$. Indeed, as the universal covering map of $\mathbf{C}^*$, its image surface is precisely M. Ignoring the fact that it does not preserve circles, let's pretend that it maps a circle packing in $\mathbf{C}$ to a circle packing in $\mathbf{C}^*$, and further, that by adjusting its period appropriately, we can obtain various combinatorics for the circle packing in $\mathbf{C}^*$. The adjustment of the period here simply means that we choose which two circles in $\mathbf{C}$ are to have identical images under the exponential map.

It is convenient to normalize the situation by basing all constructions on the regular hexagonal packing P_H in $\mathbf{C}$, which we describe shortly. One decides which circle C of P_H is to have the same image as the circle at the origin, one applies a linear map $z \mapsto \Lambda z$ which maps the center of C to $2\pi i$, and one follows this with the exponential map. Figure 5 is obtained in precisely this way; because of a judicious choice of C, it nearly replicates

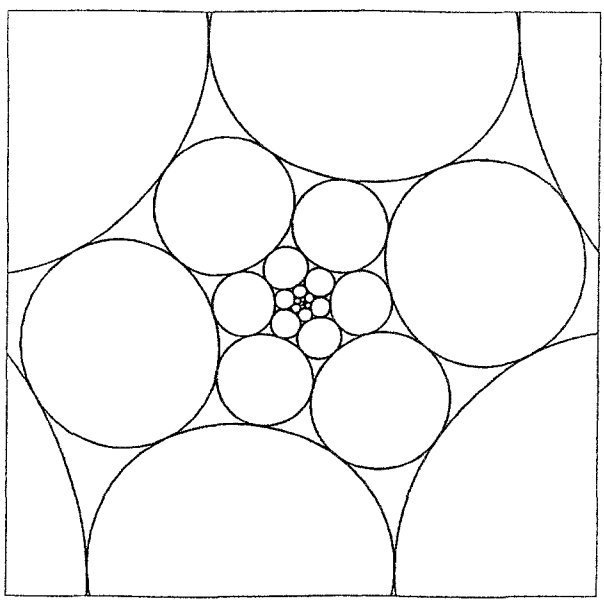

Fig. 5. Exponential image of P_H; distorted circles.

Figure 1. Unfortunately, the packed objects of Figure 5 are not circles. Our technical work involves showing how to choose Λ so that this process succeeds. We do not, however, succeed in mapping the circles of P_H to circles; rather we concentrate on the lattice of centers of P_H, showing how to map these to the appropriate centers in $\mathbf{C}^*$ using the criterion from Theorem 2.

First, the notations associated with the regular hexagonal packing P_H of $\mathbf{C}$: this packing is generated by a (non-generic) cell whose three circles are the same size, hence all its circles have the same size and their centers form a regular hexagonal lattice. We take the common radius to be 1 and assume that the fundamental quadrilateral has vertices

$$w_0 = 0,\ w_1 = 1 - \sqrt{3}\,i,\ w_2 = 2,\ w_3 = 1 + \sqrt{3}\,i. \tag{9}$$

The lattice of centers consists of integral linear combinations of w_1 and w_3 and will be denoted by H.

We define a family of linear mappings Λ involving three parameters, A, μ, and ν and their exponentials E. Each of the linear mappings is a composition of a rotation, a shear, another rotation, and a dilation. The complex parameter A ensures appropriate periodicity after we exponentiate Λ. The real parameters μ and ν are involved in the shear mapping and must have values appropriate to A; they ensure that the images of w_1, w_2, w_3 will lie on a level curve of k.

Treating A, μ, ν as free parameters for a moment, define $\Phi: x + iy \mapsto x + i(\mu x + \nu y)$, a shear. The linear mappings and associated exponentials to consider are

$$\Lambda(z) = \frac{2\pi i \Phi(|A|z/A)}{\Phi(|A|)}, \qquad E(z) = \exp\{\Lambda(z)\}. \tag{10}$$

Writing $A = |A|e^{i\theta}$, we place the following restrictions on A, to be justified later:

$$\theta \in \left[0, \frac{\pi}{6}\right] \quad \text{and} \quad |A| > \frac{2\sqrt{3}}{\sin(2\pi/3 - \theta)}. \tag{11}$$

Our technical lemma concerns the existence of appropriate values for the companion parameters μ and ν, given A. Recall the w_j's defined in (9).

LEMMA 3. *Suppose A satisfies conditions* (11). *Then there exists a unique pair of parameters $(\mu, \nu) \in \mathbf{R} \times (0, \infty)$ so that $\operatorname{Im}(\Lambda(w_j)) \in [0, \pi)$, $j = 1, 2, 3$, and so that the image points $z_1 = E(w_1)$, $z_2 = E(w_2)$, $z_3 = E(w_3)$ under the exponential map E are the vertices of a quadrilateral associated with cell continuation and satisfying* (3) *and* (8).

Conversely, given vertices z_1, z_2, z_3 *of a quadrilateral associated with cell continuation and satisfying* (3) *and* (8), *there exists a unique* A *satisfying* (11) *and unique* $(\mu, \nu) \in \mathbf{R} \times (0, \infty)$ *so that* $\mathrm{Im}(\Lambda(w_j)) \in [0, \pi)$ *and* $z_j = E(w_j)$ *for* $j = 1, 2, 3$.

The proof relies squarely on Theorem 2 and is not difficult; it is very technical, however, so it has been placed in the last section of the paper. We use its conclusions to obtain a parametrization of cell continuations: given $A \in \mathbf{C}$ satisfying (11), let μ and ν be the unique parameter values guaranteed by the lemma, and denote the associated linear map Λ by Λ_A, and exponential map E by E_A. One verifies directly that the periods of E_A are the integer multiples of A; in fact, observe for later that $|E_A(z)| = 1$ if and only if z is on the line spanned by A. By the lemma, the points $z_j = E_A(w_j)$, $j = 1, 2, 3$, along with $z_0 = 1$ are the vertices of a quadrilateral Q_A associated with cell continuation and satisfying (3) and (8). The side-pairing maps for Q_A are $f\colon z \mapsto z_1 z$ and $g\colon z \mapsto z_3 z$. These multiplicative maps lift under the logarithm to additive maps $f_0\colon z \mapsto z + \Lambda_A w_1$ and $g_0\colon z \mapsto z + \Lambda_A w_3$. Since these generate the lattice $\Lambda_A H$, one easily verifies that the orbit of centers under cell continuation of Q_A lifts under the logarithm to $\Lambda_A H$. Put another way, the points of $E_A(H)$ are precisely the centers of the circles obtained by cell continuation of Q_A.

DEFINITION. *For* $A \in \mathbf{C}^*$ *satisfying* (11), *write* Q_A *for the quadrilateral with centers* $z_j = E_A(w_j)$, $j = 0, 1, 2, 3$, *and write* P_A *for the circle packing in* $\mathbf{C}^*$ *arising from cell continuation of* Q_A.

Using these notations and applying Lemma 3, we obtain the following parameterization:

THEOREM 4. *The map* $A \to P_A$ *defines a one-to-one correspondence between complex numbers* A *satisfying* (11) *and circle packings of* $\mathbf{C}^*$ *generated by cell continuation of generic quadrilaterals satisfying* (3) *and* (8). *Every circle packing generated by cell continuation of a generic quadrilateral is equal up to similarity* (*i.e. translation, rotation, dilation, and/or conjugation*) *to a unique such* P_A.

We note the source of the conditions (11) attached to A: the precise lower bound on $|A|$ enters in the proof of Lemma 3; basically, it is necessary in order to avoid spirals which wind too tightly about the origin to be realized by packed circles. Regarding the restriction in (11) on the argument of A, it is accounted for by the six-fold rotational and the complex conjugate symmetries of H and P_H; without the restriction, distinct values of A would yield similar packings.

5. Classification of the packings P_A

With Theorem 4 we have reduced the study of cell continuation to consideration of H and the exponential maps E_A. It is important to recall that *two circles in a cell continuation are identical if and only if their centers match.* Since A is the fundamental period of E_A, we conclude that two circles in the cell continuation of Q_A are identified in P_A if and only if their centers come from lattice points of H which differ by a multiple of A. In conjunction with properties of the groups $G(Q_A)$ which we develop now, this will allow us to classify the packings P_A based on the parameter A.

We consider a generic quadrilateral Q (so that Q is not a parallelogram) which is not necessarily associated with a cell continuation. As before, we construct side-pairing maps f and g, which have a common fixed point ζ lying outside of Q, and we let $G(Q) = \langle f, g\rangle$. For brevity, we write G for $G(Q)$. We now seek conditions under which (1) G is discrete, and (2) Q is a fundamental polygon for the action of G. In deriving such conditions we assume the normalization (2) and (3). First, we prove

LEMMA 5. *G is discrete if and only if there exist integers p and q, with $q \neq 0$, such that $f^p g^q = I$.*

Proof. As $|\alpha| > 1$, f is of infinite order and $\langle f\rangle$ is discrete. If there exist integers p and q as given, then $g^q = f^{-p}$, $q \neq 0$, so that G is the finite union of the cosets $\langle f\rangle, g\langle f\rangle, \ldots, g^{q-1}\langle f\rangle$ and therefore is discrete.

Conversely, suppose that G is discrete and let $K = \{z: 1 \leqslant |z| \leqslant |\alpha|\}$. For every positive integer m there is an integer n such that $f^n g^m(1) \in K$, and by taking a subsequence we may assume that $f^n g^m(1) \to \eta$, say, and hence that $f^n g^m \to h$, where $h(z) = \eta z$. Let $\gamma_1, \gamma_2, \ldots$ be this sequence of elements $f^n g^m$: then $\gamma_m^{-1}\gamma_{m+1} \to I$ and so, by discreteness, $\gamma_m = \gamma_{m+1}$ for some m. This proves that for some p and some non-zero q, $f^p g^q = I$, completing the proof. □

As mentioned earlier, G is a two-generator abelian group and it is discrete precisely when it is of the form $\mathbf{Z} \times \mathbf{Z}_r$, and we can explain the role of r here as follows. As G is discrete, the subgroup G_R of all Euclidean rotations in G is a finite cyclic group of order r. The homomorphism $\Phi: G \to (\mathbf{R}, +)$ given by $h \mapsto \log|h(1)|$ has kernel G_R and image isomorphic to $\mathbf{Z}$ and it is easy to see that $G \simeq \Phi(G) \times G_R \simeq \mathbf{Z} \times \mathbf{Z}_r$.

We illustrate these ideas by several examples. In each of these, let Q be the quadilateral with vertices 1, 2^t, $2i$ and $2^{1+t}i$. The side-pairing maps are

$$f(z) = 2^t z,\ g(z) = 2iz,$$

and, using Lemma 5, we see that G is discrete if and only if t is rational. Assuming that $t = u/v$, where $(u, v) = \text{g.c.d}\{u, v\} = 1$, we see that $f^a g^b$ is a rotation if and only if $au + bv = 0$, and if this holds then the rotation is $z \mapsto i^b z$. Now this equation has solutions $a = -ky$, $b = ku$, for $k \in \mathbf{Z}$, and so we have the following cases:

(a) If $u \equiv 0 \bmod 4$, then $4|b$, there are no non-trivial rotations in G, and in this case $G = \mathbf{Z}$. As an example, let $t = 4/5$; then $f^5 = g^4$ and so

$$G = \langle f, g \rangle = \langle f^{-4} g^4, f^{-5} g^5 \rangle = \langle f^{-1} g \rangle = \mathbf{Z}.$$

(b) If $u \equiv 2 \bmod 4$, then b takes the values $2k$ and so $G = \mathbf{Z} \times \mathbf{Z}_2$. As an example, let $t = 2/3$; then

$$G = \langle f, g \rangle = \langle f^{-1} g, f^3 g^{-2}, f \rangle = \langle f^{-1} g, f^3 g^{-2} \rangle = \mathbf{Z} \times \mathbf{Z}_2.$$

(c) If $u \equiv 1$ or $3 \bmod 4$, then b takes all values mod 4 and so $G = \mathbf{Z} \times \mathbf{Z}_4$. As an example, let $t = 5$; then

$$G = \langle f g^{-4}, f^{-1} g^5 \rangle = \mathbf{Z} \times \mathbf{Z}_4.$$

We turn our attention now to the problem of deciding whether or not Q is a fundamental polygon for the action of G (which we now assume to be discrete). Despite the fact that G is generated by the side-pairing maps of Q, it is *not* necessarily the case that Q is a fundamental polygon: for example, let $t = 5$; then G is discrete and contains the map $f g^{-4}(z) = 2z$, and as Q has vertices 1, 32, $2i$ and $64i$ it is clear that Q and $f(Q)$ overlap. In order to solve this problem, we consider the lifted group which we mentioned briefly in the previous section.

We continue to assume that (2) and (3) hold and we note that as the origin lies outside of Q, there is a single valued logarithm on Q; we denote this by $z \mapsto L(z)$, where $L(1) = 0$. We now lift the maps f and g to

$$f_0(z) = z + L(\alpha), \; g_0(z) = z + L(\beta),$$

and it is not difficult to see that Q lifts to a curvilinear polygon Q_0 with vertices 0, $L(\alpha)$, $L(\beta)$, and $L(\alpha\beta)$, where $L(\alpha\beta) = L(\alpha) + L(\beta)$, and that f_0 and g_0 are the side-pairing maps of Q_0. We call $G_0 = \langle f_0, g_0 \rangle$ the *lifted group*. Our proof will depend on the fact that Q_0 *is* a fundamental polygon for the action of G_0; this follows (as in the standard proof of Poincaré's theorem in the theory of Kleinian groups) because $\mathbf{C}$ is simply connected, Q_0 is compact, and the G_0-images of Q_0 certainly cover a neighborhood of Q_0.

We can now give conditions for G to be discrete, and for Q to be a fundametal polygon for G, in terms of the lifted group and the cover group $\Gamma = \langle z \mapsto z + 2\pi i \rangle$.

LEMMA 6. (i) *G is discrete if and only if $\Gamma \cap G_0 \neq \{I\}$, and* (ii) *$Q$ is a fundamental polygon for G if and only if $\Gamma \subset G_0$.*

Proof. To prove (i) we have only to observe that $f^p g^q = I$ is equivalent to $\alpha^p \beta^q = 1$, and that this is equivalent to $pL(\alpha) + qL(\beta) = 2N\pi i$ for some integer N.

To prove (ii), write $\bar{E}$ for the closure of a set E (in the appropriate topology), e for the exponential map, and h_0 for the lift of a map h.

Suppose first that $\Gamma \subset G_0$; we have to prove that the G-images of $\bar{Q}$ cover the punctured plane and that distinct G-images of Q are non-overlapping. The first of these follows immediately, for

$$\bigcup_{h \in G} h(\bar{Q}) = \cup\, he(\bar{Q}_0) = \cup\, eh_0(\bar{Q}_0) = e\left(\bigcup_{h_0} h_0(\bar{Q}_0)\right) = e(\mathbf{C}) = \mathbf{C}^*,$$

where we have used the fact that Q_0 is a fundamental region for the action of G_0.

We still have to prove that distinct images of Q are non-overlapping and for this, it is sufficient to show that if Q and $h(Q)$ overlap, then $h = I$. If Q and $h(Q)$ overlap, then so do $e(Q_0)$ and $he(Q_0)$, and so too do $e(Q_0)$ and $e(h_0 Q_0)$. Using the periodicity of the exponential, this means that $h_0(Q_0)$ meets some image $\gamma(Q_0)$, where $\gamma \in \Gamma$. As $\Gamma \subset G_0$, we must have $\gamma \in G_0$ and so (as Q_0 is a fundamental region for G_0) $h_0 = \gamma$. We deduce that $h = eh_0 = e\gamma = I$ as required.

Finally, we suppose that Q is a fundamental polygon for G and we prove that $\Gamma \subset G_0$. Take any γ in Γ and any ζ in the interior of Q_0. Then $\gamma(\zeta)$ lies in some $h_0(Q_0)$ and so $\gamma(\zeta) = h_0(\zeta_1)$ for some ζ_1 in Q_0. We deduce that

$$e(\zeta) = e\gamma(\zeta) = eh_0(\zeta_1) = h(e(\zeta_1)),$$

and so Q $(= e(Q_0))$ overlaps (near $e(\zeta)$) with $h(Q)$ $(= he(Q_0))$. We deduce that $h = I$ and so $e(\zeta) = e(\zeta_1)$. As both ζ and ζ_1 lie in the fundamental region Q_0, and as L is single valued on Q_0, we have $\zeta = Le(\zeta) = Le(\zeta_1) = \zeta_1$; thus $\gamma(\zeta) = h_0(\zeta)$. Finally, as this argument holds for all points near ζ, we deduce that $\gamma = h_0$ and so, at last, $\gamma \in G_0$. The proof is complete. □

For brevity, we now identify the map $z \mapsto z + \lambda$ with λ and to complete our discussion for general quadrilaterals, let

$$\Gamma = \{2n\pi i\colon n \in \mathbf{Z}\},\ \sum = \{iy\colon y \in \mathbf{R}\}.$$

The map exp restricted to G_0 is a homomorphism of G_0 onto G with kernel $G_0 \cap \Gamma$ and so

$$G \simeq \frac{G_0}{G_0 \cap \Gamma}.$$

If G is discrete, then $G_0 \cap \Gamma$ is non-trivial. Now exp maps the complex number λ to a rotation in G if and only if $\lambda \in \Sigma$, and so finally, we see that $G = \mathbf{Z} \times \mathbf{Z}_r$, where

$$\frac{G_0 \cap \Sigma}{G_0 \cap \Gamma} \simeq \mathbf{Z}_r.$$

We now wish to apply these ideas to the projection E_A of the hexagonal lattice H as described in the previous section; that is, Q is the quadrilateral Q_A associated with a cell continuation. Here we have interposed—before the exponential—the $\mathbf{R}$-linear automorphism Λ_A of $\mathbf{R} \times \mathbf{R}$ satisfying:

(i) $\Lambda_A(z) \in \langle 2\pi i \rangle$ if and only if $z \in \langle A \rangle$;

(ii) $\Lambda_A(z)$ is purely imaginary if and only if $z \in \{tA: t \in \mathbf{R}\}$.

Therefore, $E_A(H)$ and H play the roles of $G = G(Q_A)$ and its lifted group G_0, respectively, $\Gamma = \langle A \rangle$, and $\Sigma = \{tA: t \in \mathbf{R}\}$. The methods used above now yield $G \simeq H/(H \cap \Gamma)$. We arrive at the following trichotomy based on the choice of A:

(I) $A \in H$: Here, $\Gamma \subset H$, and by Lemma 6, Q_A is fundamental for $G(Q_A)$. We conclude that any two circles obtained by cell continuation of Q_A will either have disjoint interiors or will be identical. In this case (and only this case), the associated pattern P_A is a *coherent* circle packing of $\mathbf{C}^*$.

(II) $nA \in H$ for integer $n > 1$: Assume n is the smallest such integer. Then $\Gamma \cap H$ is a subgroup having finite index n in Γ, and by Lemma 6, $G(Q_A)$ is discrete but Q_A is not fundamental. One can see, in fact, that P_A represents the projection to $\mathbf{C}^*$ of a spiral circle packing on an n-sheeted covering of $\mathbf{C}^*$—one might think of it as an 'n-layered' spiral circle packing.

(III) Otherwise: $\Gamma \cap H = \{I\}$ and $G(Q_A)$ is not discrete. The spiral packing P_A has no coherency whatever. No two points of H have the same image under E_A, so the circles of P_A are in one-to-one correspondence with H and their centers form a dense set in the plane.

Among the coherent circle packings P_A, the associated group $G(Q_A)$ gives us one further piece of data for classification. Namely,

$$G(Q_A) \simeq \mathbf{Z} \times \mathbf{Z}_r, \mathbf{Z}_r \simeq \frac{H \cap \Sigma}{H \cap \Gamma}.$$

It is not difficult to compute r: Since P_A is coherent, $A \in H$. Write $A = pw_1 + qw_2$ (by the normalization of (11), $1 \leqslant p \leqslant q \leqslant 2p$). Then $H \cap \Sigma$

is generated by $(p/r)w_1 + (q/r)w_3$, where $r = (p, q)$, and so

$$G(Q_A) \simeq \mathbf{Z} \times \mathbf{Z}_r,\ r = (p, q).$$

This can be observed in the packing P_A, which will be invariant under the rotation $z \mapsto e^{2\pi i/r}z$. Moreover, these are the only rotational symmetries, for recall that two circles of P_A will have the same radius if and only if their centers have the same modulus. Thus, the rotated images of C_0 have centers associated with $H \cap \Sigma$, and there are precisely r of these, modulo Γ. Several examples of coherent spirals are illustrated in Figure 6 and discussed in Section 7; we will be noting the rotational symmetries which they exhibit.

A final point about coherent spirals and the conditions (11) attached to A: The parameters satisfying (11) are strictly outside the regular hexagon which is centered at the origin and has vertex at $x = 4$ on the real axis. Superimposed on P_H, that hexagon passes through the centers of the circles which are two generations from the one at the origin; in particular, one can easily verify that such circles are too close to the circle at the origin to be identified with it in a spiral.

6. Characterization of the coherent circle packings

The circle packings P_A with $A \in H$ are coherent. One might ask whether there exist any other coherent hexagonal circle packings. The answer is no.

THEOREM 7. *Every coherent hexagonal circle packing P in the plane is identical, up to similarity, with the regular hexagonal circle packing P_H or with a spiral circle packing P_A for some $A \in H$ satisfying* (11). *In particular, these packings P_A provide an infinite family of combinatorially distinct coherent circle packings of* $\mathbf{C}^*$.

Proof. Recall that P is a coherent hexagonal circle packing if its circles have pairwise disjoint interiors and each is tangent to and surrounded by six others; its *carrier* is the union of the circles, their interiors, and the triangular interstices formed by mutually tangent triples of circles. Connecting the centers of pairs of tangent circles by Euclidean line segments yields a locally finite triangulation of the carrier; this geometric object corresponds to an abstract (orientable) simplicial 2-complex which we will denote by K_P. If it should be the case that $P = P_A$, then we write K_A for its complex. (A refers throughout this section to a point in H satisfying (11).)

The combinatorics of P are encoded in K_P, and it turns out that they are all-important.

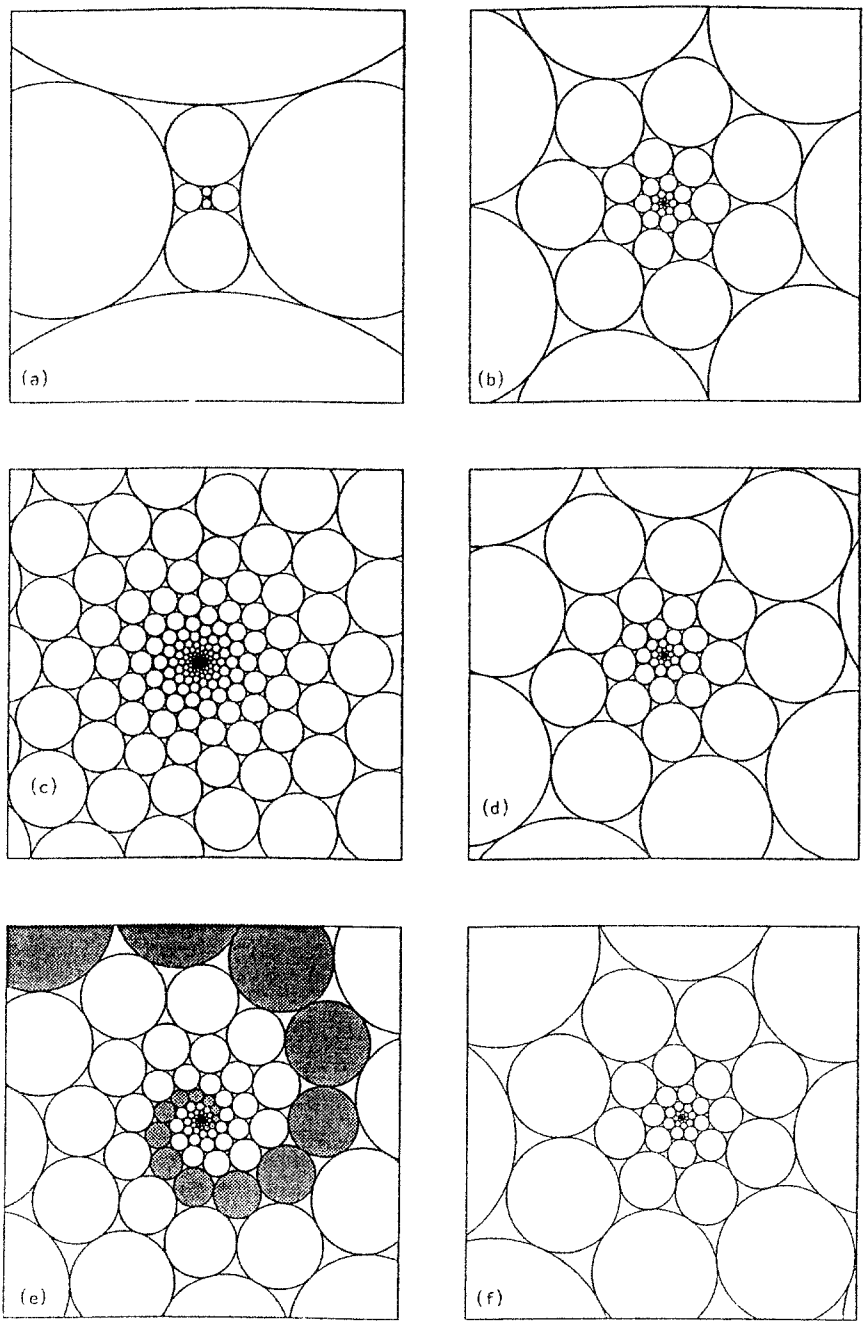

Fig. 6. Examples of coherent spiral circle packings.

LEMMA 8. *Coherent hexagonal circle packings P and P' are identical up to similarity if and only if their complexes K_P and $K_{P'}$ are simplicially equivalent.*

Proof of lemma. Sufficiency is obvious; necessity lies much deeper. Assume K_P and $K_{P'}$ are simplicially equivalent:

First, note that because the complex K_P is hexagonal, it is known to be intrinsically flat by results in [BSt]—in the language there, K_P is a complex of 'parabolic type'. As a consequence, results from the theory of quasiregular mappings imply that the carrier of any coherent circle packing with the combinatorics of K_P must equal the whole plane or the once-punctured plane. (See Example 4, Proposition 1, and the proof of Proposition 1 in [BSt].) In the former case, K_P is simply connected, while in the latter it is a topological annulus. In particular, the equivalence of K_P and $K_{P'}$ implies that P and P' have homeomorphic carriers.

We can dispense first with the case that their carriers are the whole plane: With simple connectivity, one easily verifies that the complex is simplicially equivalent to that underlying the regular hexagonal circle packing, which we will denote K_H. A uniqueness result of Sullivan (see the Appendix of [RS]) implies that any coherent circle packing with complex K_H is similar to P_H, the regular hexagonal circle packing. If K_P and $K_{P'}$ are simply connected, then, both are similar to P_H, hence to one another.

Assume henceforth that the carriers of P and P' are once-punctured planes; we may assume both omit the point 0. Here we rely on a theorem of O. Schramm which considerably extends Sullivan's uniqueness result: Theorem 1.1 of [Sc] says that if two coherent circle packings in the plane have the same combinatorics and one has a carrier omitting at most a countable number of points, then the two circle packings are Möbius transformations of one another. Here, simplicial equivalence of K_P and $K_{P'}$ is precisely the meaning of 'combinatorial equivalence' and their carriers omit at most one point, so Schramm's results implies that they are identical up to similarity. This proves the lemma. □

Our proof of Theorem 7 now reduces to purely combinatoric considerations. It is enough to prove these two statements:

(i) Given A and A', the complexes K_A and $K_{A'}$ are simplicially equivalent only if $A = A'$.

(ii) If P is a hexagonal circle packing with carrier $\mathbf{C}^*$, then there exists an A so that K_P and K_A are simplicially equivalent.

To address these, we use the complex K_H associated with P_H; note that this is simplicially equivalent to the geometric triangulation of the plane,

which we denote by $\mathcal{T}$, consisting of equilateral triangles formed by connecting the centers of tangent circles of P_H. When the carrier of P omits a point of the plane, then K_P is a topological annulus, and it is straightforward to prove that K_H is its simplicial universal covering complex; that is, there is a (orientation-preserving or reversing) covering map of K_H onto K_P which carries simplexes to simplexes. The associated covering group Σ_P is a subgroup of $\mathrm{Aut}(K_H)$, the simplicial automorphism group of K_H, and two complexes K_P are simplicially equivalent if and only if these groups Σ_P are conjugate. Since K_P is an annulus, Σ_P will be an infinite cyclic group generated by a fixed-point-free, orientation-preserving element.

The automorphisms of K_H are more easily understood in the concrete setting of $\mathcal{T}$: the fixed-point-free, oriented, infinite order ones are translations $\tau_V: z \mapsto z + V$, where the complex number V represents the displacement vector between two vertices of $\mathcal{T}$ (i.e. $V \in H$). Using symmetries of $\mathcal{T}$ (namely, conjugating by automorphisms fixing 0), we see that τ_V is conjugate to some $\tau_{V'}$, where $V' \in H$ satisfies $\mathrm{Arg}(V') \in [0, \pi/6]$. Moreover, since distinct points of H in this sector cannot be conjugate in $\mathrm{Aut}(K_H)$, V' is unique. We conclude that each P is associated with a unique point $V \in H$ satisfying $\mathrm{Arg}(V) \in [0, \pi/6]$, where τ_V generates the covering group Σ_P.

Now, consider one of our packings P_A. The associated exponential map E_A is a group homomorphism mapping H onto the (multiplicative) group J of centers of P_A. Moreover, using the fact that $E_A(w_j) = z_j$, $j = 0, 1, 2, 3$, one can verify that E_A maps the centers of mutually tangent triples of circles of P_H to the centers of mutually tangent triples of circles in P_A. It is immediate that $E_A | H$ induces a simplicial covering map of K_H onto K_A. Since A is the fundamental period of E_A, the associated covering group is generated by τ_A. In particular, since $A \in H$ satisfies $\mathrm{Arg}(A) \in [0, \pi/6]$, the result (i) follows from the last statement of the previous paragraph. As for (ii), we need only show that given P, the point V whose translation τ_V generates Σ_P is one of our allowable parameters A. Every $V \in H$ with $\mathrm{Arg}(V) \in [0, \pi/6]$ may be written uniquely as $V = pw_1 + qw_2$ for integers p, q satisfying $0 < p \leqslant q \leqslant 2p$. One easily checks that if $p \geqslant 2$, then $|V| > 4\cos(\mathrm{Arg}(V))$, and setting $A = V$, we conclude that $P = P_A$. That leaves only two cases to consider: $(p, q) = (1, 1) \Rightarrow V = 2$ and $(p, q) = (1, 2) \Rightarrow V = 3 + \sqrt{3}\,i$. In the first case, two circles tangent to one another in P_H are to be identified in P, which is clearly impossible. In the second case, two circles tangent to a common third circle are to be identified. A moment's reflection confirms that no packing spiraling around the origin can accomplish this either. Thus these two cases don't arise, and we have proven (ii). □

7. Concluding remarks

(a) Several examples of coherent spiral circle packings are illustrated in Figure 6; Table I provides the various parameters associated with these and with the spiral of Figure 1. All have fundamental quadrilaterals Q in the normlized position, i.e. satisfying (3) and (8).

Figure 6(a) is one of the tighter spiral packings. Figures 6(a)–(c) illustrate the 'endpoint' cases mentioned at the end of Section 3; (a) and (c) are in Case I of the proof of Lemma 3 while (b) is in Case II. In the typical spiral packing, the orbit of a circle under each of $\langle f \rangle$, $\langle g \rangle$, and $\langle fg \rangle$ will be a chain of tangent circles which spirals out to ∞ in one direction and in to 0 in the other. In Figure 6(e), one such spiral path has been shaded; this particular spiral is an orbit of $\langle fg \rangle \subset G(Q)$. There are exceptions, of course: the orbits of $\langle f \rangle$ lie along rays in Figure 6(a) and the orbits of $\langle fg \rangle$ are 7-circle rings in 6(b).

Recall from Section 5 that $G(Q) \simeq \mathbf{Z} \times \mathbf{Z}_r$. The values of r can be seen in the rotational symmetry of the spirals. For instance, Figure 1 and Figure 6(a) have 2-fold symmetry, 6(b) has 7-fold symmetry, 6(c) has 9-fold symmetry, 6(d) has 3-fold symmetry, and 6(e) has 4-fold symmetry. Figure 6(f) displays no rotational symmetry; in fact, the whole packing can be seen to consist of a single spiral, implying that its group $G(Q)$ is cyclic. The information on rotational symmetry can be verified with the data in our table since r is the greatest common divisor of the integers p and q in the representation $A = pw_1 + qw_2$.

(b) In Table I, the reader interested in experimenting with spirals can obtain approximate values of parameters associated with the various figures of the paper. It gives the integers p, q, the vector $A = pw_1 + qw_2$ and parameters μ, ν for the exponential map, the centers z_1, z_3, and the four radii R_0, R_1, R_2, R_3 for the quadrilateral Q. It is perhaps easiest to generate new patterns using the ratios R_1/R_0 and R_2/R_0 as parameters. To get coherent and/or n-sheeted spirals, it suffices to manipulate the parameters until some two (any two!) circles end up with the same center. However, even with a computer program to facilitate the work, doing this in an *ad hoc* way is rather more difficult than one might suspect.

(c) There is some pretty geometry associated with the level curves of the function $k(z) = (1 + |z|)/|1 - z|$ of Section 3, and circles enter in an intriguing new way.

As noted earlier, the level curves of k are known as 'Ovals of Descartes'. (Actually, Cartesian ovals come in conjugate pairs; we have as yet seen no geometric significance in regard to circle packings for the conjugate family.)

TABLE I

	p/q	A	μ/ν	z_1/z_3	$R_0/R_1/R_2/R_3$
Fig. 1	4	$10 + 2\sqrt{3}\,i$	0.00033329698	$3.37 + 0.76i$	0.55929
	6		1.06430488878	$0.27 + 0.34i$	1.93464
					0.24453
					0.84585
Fig. 6(a)	2	$6 + 2\sqrt{3}i$	0	8.35	0.78615
	4		1.17022321709	$0.34i$	6.56625
					0.27201
					2.27201
Fig. 6(b)	7	14	0	$2.02 + 0.97i$	0.43388
	7		1.03549053886	$0.4 + 0.19i$	0.97039
					0.19399
					0.43388
Fig. 6(c)	9	$27 + 9\sqrt{3}\,i$	0	1.5	0.20017
	18		1.00683408652	$0.77 + 0.28i$	0.30036
					0.16341
					0.24520
Fig. 6(d)	6	$15 + 3\sqrt{3}\,i$	0.00006362805	$2.19 + 0.33i$	0.38553
	9		1.02714766087	$0.48 + 0.33i$	0.85668
					0.22640
					0.50308
Fig. 6(e)	8	$20 + 4\sqrt{3}\,i$	0.0000198988	$1.79 + 0.2i$	0.29251
	12		1.01500905487	$0.61 + 0.29i$	0.52861
					0.19715
					0.35629
Fig. 6(f)	7	$15 + \sqrt{3}\,i$	2.1963612	$2.08 + 0.71i$	0.40421
	8		1.1033491	$0.44 + 0.24i$	0.88778
					0.44598
					0.20305

More interesting than the nomenclature is the fact that the level curves of k are the images of circles under the squaring map $s: z \mapsto z^2$. In particular, one can check that if C is a circle in the half plane $x > 0$ which is orthogonal to the real axis and to the unit circle $\{|z| = 1\}$, then $s(C)$ is a level curve of k; and all level curves of k arise in this way. Now, if $A \in H$ satisfies (11) and it happens that $A/2 \in H$, then applying s to the whole configuration P_A yields a packing of $\mathbf{C}^*$ by Ovals of Descartes! Moreover, since any two circles of P_A are images of one another under a complex multiplication, these ovals are all similar to one another. Figure 7 provides an illustration of one of these pleasing patterns, obtained by squaring the configuration of Figure 1.

(d) There are more abstract methods for generating spiral circle packings:

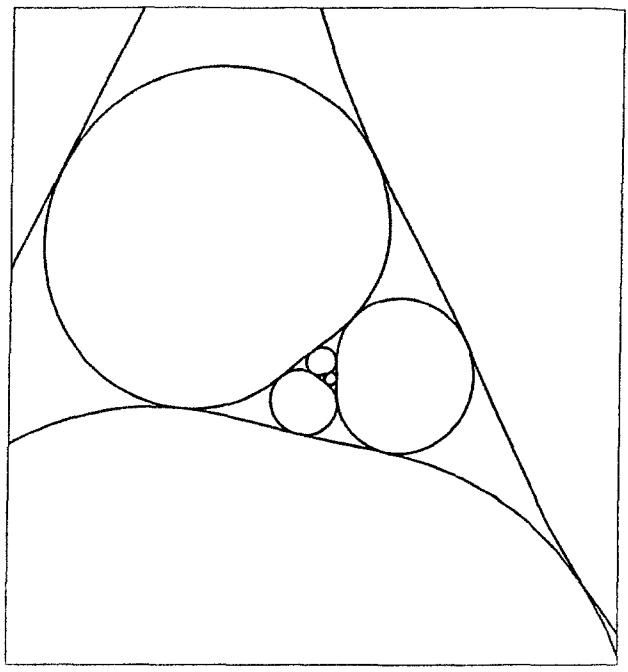

Fig. 7. A spiral packing by Ovals of Descartes.

Figure 8 illustrates a coherent spiral packing in $\mathbf{C}^*$ whose combinatorics are non-hexagonal. This particular example was chosen because it exhibits symmetry involving a fundamental quadrilatral Q (shaded in the figure), so parts of our analysis remain applicable: there is an underlying discrete group action on the packing generated by side pairing maps—the shaded circles having eight neighbors comprise one orbit and the rest comprise another—and hence the relationship (1) follows for the radii of the four corner circles of Q. However, missing are the elementary self-generating feature exhibited by cell continuation, the beautiful geometry associated with the Ovals of Descartes, the explicit exponential mappings, and the continuous parametrizaton of (mostly non-coherent) packings. Indeed, the technique we used to generate Figure 8 and which works in fairly general circumstances (a technique suggested to the authors by a referee) starts by prescribing the desired combinatorics and then employs finite exhaustion, the Koebe–Andreev–Thurston theorem, the Ring lemma, and finally a geometric diagonalization. It is restricted to generation of coherent packings, so in the hexagonal case one can establish Theorem 7, but not Theorem 4.

(e) *Added in revison:* See [RK] for an application of spiral circle packings

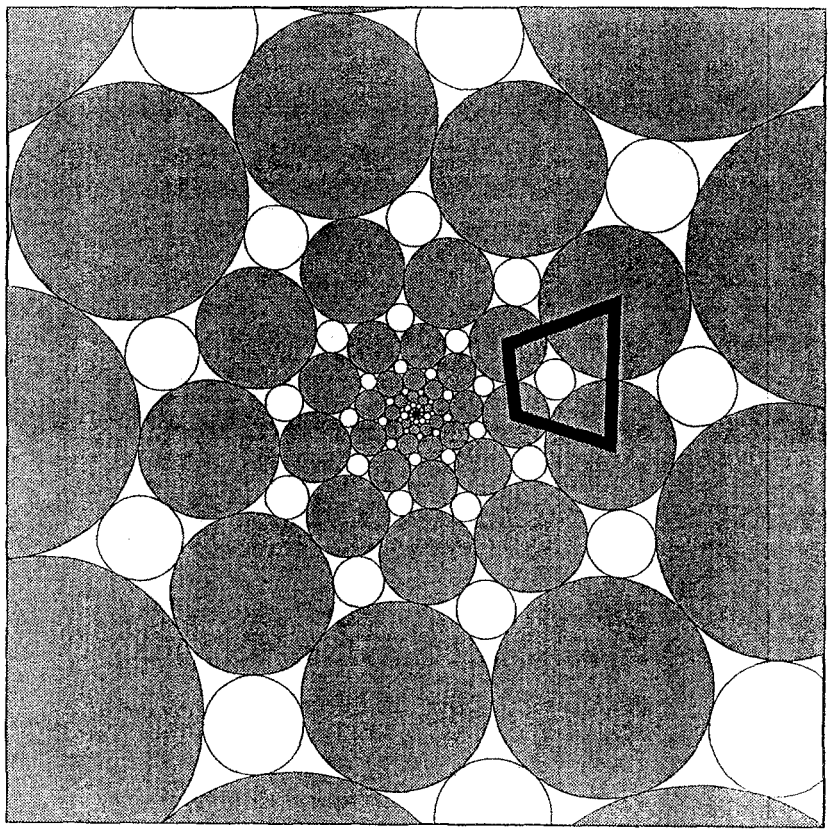

Fig. 8. A non-hexagonal coherent spiral packing.

in *phyllotaxis,* the study of geometric patterns in plants. The generic case in [RK] involves quadrilateral interstices such as those formed by the shaded circles of Figure 8. Nonetheless, as noted in (d) above, our analysis using side-pairing maps continues to apply. The 'close-packing' patterns in [RK] are among our coherent hexagonal spiral packings.

8. Proof of lemma 3

Assume first that $A = |A|e^{i\theta}$ is fixed and satisfies (11), and the points z_1, z_2, z_3 designate the images of w_1, w_2, w_3 under the exponential E_A. The parameters $(\mu, \nu) \in \mathbf{R} \times (0, \infty)$ are to be chosen so that

$$\text{(12)} \qquad \mathrm{Im}(\Lambda_A(w_j)) \in [0, \pi), \; j = 1, 2, 3,$$

and so that the z_j are vertices of a quadrilateral associated with cell continuation. (Uniqueness will follow from the proof of the converse.)

In light of Theorem 2, we will concentrate on choosing μ and v so that $k(z_1) = k(z_2) = k(z_3)$. Noting that $z_2 = z_1 z_3$, we break this equality into the two identities

$$(13) \qquad \text{(i)} \ \frac{1+|z_1 z_3|}{|1-z_1 z_3|} = \frac{1+|z_3|}{|1-z_3|} \qquad \text{(ii)} \ \frac{1+|z_1|}{|1-z_1|} = \frac{1+|z_3|}{|1-z_3|}.$$

Switching to more convenient parameters s, t related to μ, v, (13)(i) and (ii) will lead to equations $f(s,t) = 0$ and $g(s,t) = 0$ which must be solved simultaneously. The expressions get a little complicated and there are some endpoint cases to consider, but the arguments are otherwise straightforward. Start by defining several recurring constants:

$$\gamma = \frac{2\pi}{3} - \theta,\ a = -\sin\gamma + \sqrt{3}\cos\gamma,\ b = \sin\gamma + \sqrt{3}\cos\gamma,\ c = \frac{2\pi}{|A|},$$

$$p = \frac{-a|A|}{2\sqrt{3}}, \qquad q = \frac{|A|(b-a)}{2\sqrt{3}}.$$

Under conditions of (11), $a \leqslant a+b \leqslant 0 \leqslant b$, $\gamma \in [\pi/2, 2\pi/3]$, $p \leqslant q \leqslant 2p$, $q > 2$, and $p > 1$; note that p, q are generally not integers.

For parameters $\mu \in \mathbf{R}$ and $v > 0$, the exponential function $E = E_A$ is defined in (10). The values of interest are $z_1 = E(w_1) = E(1 - \sqrt{3}\,i)$ and $z_3 = E(w_3) = E(1 + \sqrt{3}\,i)$, and they are given explicitly by

$$E(w_1) = \exp\left\{c(b-a)\left(\frac{v}{1+\mu^2}\right)\right\} \cdot \exp\left\{-ci\left(\frac{a+b}{\sqrt{3}} + (b-a)\left(\frac{\mu v}{1+\mu^2}\right)\right)\right\},$$

$$E(w_3) = \exp\left\{ca\left(\frac{v}{1+\mu^2}\right)\right\} \cdot \exp\left\{ci\left(\frac{2b-a}{\sqrt{3}} - a\left(\frac{\mu v}{1+\mu^2}\right)\right)\right\}.$$

However, it is convenient to introduce new parameters and some auxiliary functions:

$$s = \frac{\mu v}{1+\mu^2}, \quad t = \exp\left\{\frac{cv}{1+\mu^2}\right\},$$

$$h_1(s) = -c\left(\frac{a+b}{\sqrt{3}} + (b-a)s\right), \quad h_2(s) = c\left(\frac{b-2a}{\sqrt{3}} - bs\right),$$

$$h_3(s) = c\left(\frac{2b-a}{\sqrt{3}} - as\right).$$

Note that $h_j(s)$ is just $\mathrm{Im}(\Lambda_A(w_j))$. In terms of these variables and functions, we have $z_1 = t^{(b-a)}e^{ih_1(s)}$, $z_3 = t^a e^{ih_3(s)}$, $z_2 = t^b e^{ih_2(s)}$, and a computation shows that $ph_1(s) + qh_3(s) = 2\pi$, $s \in \mathbf{R}$. Define

$$s_0 = \frac{2b-a}{a\sqrt{3}}, \quad s_1 = \frac{a+b}{\sqrt{3}(a-b)}. \tag{14}$$

Then $s_0 < 0 \leqslant s_1$ and $h_1(s_0) = 2\pi/p$, $h_1(s_1) = 0$, while $h_3(s_0) = 0$, $h_3(s_1) = 2\pi/q$. The functions $h_j(s)$ are linear, with h_1 decreasing and h_3 increasing. We will limit our search for the parameter s to the interval $s \in [s_0, s_1]$.

We now define the auxiliary functions associated with the important equalities (13). First define

$$X(s) = \cos[h_1(s)] = \frac{\Re z_1}{|z_1|}, \quad Y(s) = \cos[h_2(s)] = \frac{\Re z_2}{|z_2|},$$

$$Z(s) = \cos[h_3(s)] = \frac{\Re z_3}{|z_3|}.$$

By moving everything to the left side in (13)(i), breaking into real and imaginary parts, and reorganizing, we obtain the auxiliary function

$$f(s,t) = (1+Y)t^b - (1+Z)t^{2b+a} + 2(Y-Z)t^{a+b} - (1+Z)t^a + (1+Y)t^{b+2a}.$$

Identity (13)(i) is equivalent to $f(s,t) = 0$. Working likewise with (13)(ii) we obtain the auxiliary function

$$g(s,t) = (1+Z)t^{2b-a} - (1+X)t^{b-a} - 2(X-Z)t^b - (1+X)t^{b+a} + (1+Z)t^a.$$

Identity (13)(ii) is equivalent to $g(s,t) = 0$. We will need to put some effort into analysing these auxiliary functions in order to find simultaneous solutions. The analysis varies with γ, and we begin with the simpler endpoint cases.

CASE I. $\gamma = \pi/2$: Here $a = -1$, $b = 1$, $2p = q > 2$, $s_0 = -\sqrt{3}$, and $s_1 = 0$. We have $f(s,t) = (Y-Z)(t+2+t^{-1})$, so f can vanish only if $Y(s) = Z(s)$,

hence only if $h_1(s) = 0 (\mathrm{mod}\, 2\pi)$. With the restriction $s \in [s_0, s_1]$, this implies $s = 0$. Now

$$g(0,t) = (1+Z)t^3 - 2t^2 - 2(1-Z)t - 2 + (1+Z)t^{-1}.$$

Since $h_3(0) = 2\pi/q < \pi$, $-1 < Z(0) < 1$. One can verify that $g(0,1) < 0$ and $g(0,t) > 0$ for t large; therefore there exists a value $\tau > 1$ with $g(0,\tau) = 0$. Concluding this case, we see that $(s,t) = (0,\tau)$ is the unique simultaneous solution of $f(s,t) = 0$ and $g(s,t) = 0$ for $s \in [s_0, s_1]$.

CASE II. $\gamma = 2\pi/3$: Here $a = -\sqrt{3}, b = 0$, $p = |A|/2 = q > 2$, $s_0 = -1/\sqrt{3}$, and $s_1 = 1/\sqrt{3}$. We have $g(s,t) = (Z - X)(t^{\sqrt{3}} + 2 + t^{-\sqrt{3}})$, so g can vanish only if $X(s) = Z(s)$, hence only if $\cos(h_1(s)) = \cos(h_3(s))$. Since $h_1(s)$, $h_3(s) \in [0, \pi]$ for $s \in [s_0, s_1]$, this implies again that $s = 0$. We have

$$f(0,t) = (1+Y) + (2Y - 4Z - 2)t^{-\sqrt{3}} + (1+Y)t^{-2\sqrt{3}}.$$

Since $Z(0) > Y(0) > -1$, $f(0,1) < 0$, and $f(0,t) > 0$ for t large; therefore there exists a value $\tau > 1$ with $f(0,\tau) = 0$. Concluding case II, we see that $(s,t) = (0,\tau)$ is the unique simultaneous solution of $f(s,t) = 0$ and $g(s,t) = 0$ for $s \in [s_0, s_1]$.

CASE III. $\gamma \in (\pi/2, 2\pi/3)$: Here $a < a + b < 0 < b$, $2 < q$, $1 < p < q < 2p$, and s_0, s_1 are as given in (14). Things become more complicated now since we must work with both s and t.

We consider $s \in [s_0, s_1]$, but in fact we can first eliminate part of this interval. Let

$$\delta_1 = \frac{\sqrt{3}b}{(2a-b)} \quad \text{and} \quad \delta_2 = \frac{1}{b}\left(\frac{b-2a}{\sqrt{3}} - \frac{|A|}{2}\right).$$

Then $h_2(\delta_2) = \pi$ and $h_1(\delta_1) = h_3(\delta_1)$. In particular, $\delta_1 \in (s_0, s_1)$. Moreover, $q > 2$ implies $\delta_2 < s_1$. Let $\delta = \max\{\delta_1, \delta_2\}$. Then $\delta \in (s_0, s_1)$ and we restrict our search to the interval $[\delta, s_1]$. Since $-1 < X(\delta) \leqslant Z(\delta)$ (and recalling that we require $t > 1$),

$$g(\delta, t) \geqslant (1 + X(\delta))(t^{b-a} - t^a)(t^b - 1) > 0;$$

so $s = \delta$ is out. Also, note that $X(s_1) = 1$, so $Z(s_1) = Y(s_1)$ and

$$f(s_1, t) = (1+Y)(t^b - t^a)(1 - t^{b+a}) > 0; \tag{15}$$

so $s = s_1$ is also out.

We can restrict attention, then, to $s\in(\delta, s_1)$. For this interval we have

$$-1 < Y(\delta) < Y(s) < Z(s) < X(s) < 1,$$

$$X'(s) > 0, \quad Y'(s) > 0, \quad Z'(s) < 0.$$

First an investigation of the roots of f: Fix $s\in(\delta, s_1)$. Define the auxiliary functions $F(t) = t^{-b-2a}f(s, t)$, and $\mathscr{F}(t) = t^{2a+1}F'(t)$. Note that $F(1) = 4(Y - Z) \leqslant 0$, $\mathscr{F}(1) = 4a(Z - Y) \leqslant 0$, and $\lim_{t\to\infty} F(t) = \lim_{t\to\infty} \mathscr{F}(t) = \infty$. Moreover,

$$\mathscr{F}'(t) = (a^2 - b^2)(1 + Z)(t^{b+a-1} + t^{a-b-1})$$
$$-2a^2(Y - Z)t^{a-1} > 0.$$

We see that $\mathscr{F}$ has a unique root t_1 in $[1, \infty)$ with $t_1 > 1$, and consequently that F has a unique root $t_0 > t_1$. In particular, $t_0 > 1$ is a root of f. Defining $t(s) = t_0$, we can conclude that $(s, t(s))$ is the unique solution to $f(s, t) = 0$ in $(\delta, s_1) \times (1, \infty)$. Note that the partial derivative

$$f_t(s, t(s)) = \frac{dF}{dt}(t_0)t_0^{2a+b} > 0$$

because

$$\frac{dF}{dt}(t_0) > 0.$$

The fact that $Z'(s) < 0$ and $Y'(s) > 0$ and a computation show that $f_s(s, t(s)) > 0$. Applying the implicit function theorem yields

$$\frac{dt}{ds}(s) = -\frac{f_t(s, t(s))}{f_s(s, t(s))} < 0.$$

Therefore, $t:(\delta, s_1) \to (1, \infty)$ is strictly decreasing. Lastly, we must consider the behavior at the endpoints. By monotonicity, $\lim_{s\downarrow\delta} t(s)\in(1, \infty]$ and $\lim_{s\uparrow s_1} t(s) = T_0$ for some $T_0 \geqslant 1$. By continuity, $f(s_1, T_0) = 0$. Since $Z(s_1) = Y(s_1) > -1$, (15) shows that $T_0 = 1$. Moreover, if $\delta = \delta_2$ then $\lim_{s\downarrow\delta} t(s) = \infty$, for otherwise there exists $\tilde{T}_0 = \lim_{s\downarrow\delta} t(s)\in(1, \infty)$ and by continuity, $f(\delta_2, \tilde{T}_0) = 0$. But $-1 = Y(\delta_2) < Z(\delta_2) < X(\delta_2)$, so

$$f(\delta_2, \tilde{T}_0) = -(1 + Z)\tilde{T}_0^{2b+a} + 2(-1 - Z)\tilde{T}_0^{a+b} - (1 + Z)\tilde{T}_0^{a} < 0.$$

Writing $\tau_f(s)$ for the function $t(s)$, we may now summarize:

SUMMARY. *There exists a continuous, strictly decreasing function* τ_f: $(\delta, s_1) \to (1, \infty)$ *so that* $f(s, \tau_f(s)) = 0$, $s \in (\delta, s_1)$, *with* $\lim_{s \uparrow s_1} \tau_f(s) = 1$, $\lim_{s \downarrow \delta} \tau_f(s) \in (1, \infty]$, *and* $\lim_{s \downarrow \delta} \tau_f(s) = \infty$ *if* $\delta = \delta_2$.

A parallel analysis can be carried out for the auxiliary function g. We leave the computations to the interested reader and only summarize:

SUMMARY. *There exists a continuous, strictly increasing function* $\tau_g: (\delta, s_1) \to (1, \infty)$ *so that* $g(s, \tau_g(s)) = 0$, $s \in (\delta, s_1)$, *with* $\lim_{s \uparrow s_1} \tau_g(s) \in (1, \infty]$, $\lim_{s \downarrow \delta} \tau_g(s) = 1$, *and* $\lim_{s \downarrow \delta} \tau_g(s) = 1$ *if* $\delta = \delta_1$.

The endpoint behavior, the continuity, and the fact τ_f is decreasing while τ_g is increasing imply existence of a unique point $s \in (\delta, s_1)$ so that $\tau_f(s) = \tau_g(s) = \tau \in (1, \infty)$. This completes case III.

With these three cases, we have shown that any A satisfying (11) gives rise to a pair $(s, t) \in [s_0, s_1] \times (1, \infty)$ which is a simultaneous solution of equations $f(s, t) = 0$ and $g(s, t) = 0$. That is, z_1, z_2, z_3 satisfy (13)(i) and (ii) and, *via* Theorem 2, are vertices of a quadrilateral associated with cell continuation. For the solutions (s, t), a check in each of the three cases confirms that $h_j(s) \in [0, \pi)$, $j = 1, 2, 3$, giving condition (12). Confirmation of normalizations (3) and (8) is left to the reader. Values μ, ν corresponding to s, t are easily computed, so this completes proof of the existence in the direct implication of the lemma.

For the converse, suppose z_1, z_2, z_3 and $z_0 = 1$ are vertices of a quadrilateral associated with cell continuation and satisfying normalizations (3) and (8). Observe that by Theorem 2 and properties of the level sets of k,

$$\frac{1}{|z_1|} \leqslant |z_3| \leqslant \left(\frac{1}{|z_1|}\right)^{1/2}. \tag{16}$$

Also, writing $z_1 = e^{\alpha_1 + i\beta_1}$, $z_3 = e^{\alpha_3 + i\beta_3}$, with $\beta_1, \beta_3 \in [0, \pi)$, the normalizations imply $\alpha_1 > 0 > \alpha_3$ and $0 \leqslant \beta_1 \leqslant \beta_3 \leqslant \beta_1 + \beta_3 < \pi$. By (16), $-2 \leqslant \alpha_1/\alpha_3 \leqslant -1$.

For $\gamma \in [\pi/2, 2\pi/3]$, $c \in (0, \infty)$, $s \in \mathbf{R}$, define the constants a, b and functions $h_j(s)$, $j = 1, 2, 3$, as earlier. Suppose we find unique values γ, c, s, t such that:

(i) $(\gamma, c, s, t) \in [\pi/2, 2\pi/3] \times (0, \infty) \times \mathbf{R} \times (0, \infty)$,

(ii) $A = (c/2\pi)e^{i(2\pi/3 - \gamma)}$ satisfies (11), and

(iii) $z_1 = t^{(b-a)8} e^{ih_1(s)}$ and $z_3 = t^a e^{ih_3(s)}$, $h_1(s) = \beta_1$ and $h_3(s) = \beta_3$.

Then the proof will be completed, because, with μ, ν related to s, t as earlier, we will have $h_j(s) = \mathrm{Im}(\Lambda_A(w_j))$ and $E_A(w_j) = z_j$, $j = 1, 2, 3$.

One first verifies that there is a unique $\gamma_0 \in [\pi/2, 2\pi/3]$ which satisfies

$$\frac{\alpha_1}{\alpha_3} = \frac{2\sin\gamma}{-\sin\gamma + \sqrt{3}\cos\gamma}.$$

It follows that c, s, t are defined uniquely by

$$c = \frac{\sin\gamma_0}{\sqrt{3}}\left[\beta_3 + \beta_1\left(\frac{\sin\gamma_0 - \sqrt{3}\cos\gamma_0}{2\sin\gamma_0}\right)\right],$$

$$s = -\frac{\beta_1 + 2c\cos\gamma_0}{2c\sin\gamma_0}, \qquad t = \exp\left\{\frac{\alpha_1}{2\sin\gamma_0}\right\}.$$

It is easy to check that (i) and (iii) are satisfied. Taking $\gamma = \gamma_0$, define A as in (i). We need only verify the condition on $|A|$ in (11). Define p and q as before and observe that $0 < p \leqslant q \leqslant 2p$ and $p\beta_1 + q\beta_3 = 2\pi$. This last equation, the requirement that $0 \leqslant \beta_1 + \beta_3 < \pi$, and the fact that $\beta_1 \geqslant 0$ give

$$\left(1 - \frac{p}{q}\right)\beta_1 < \left(1 - \frac{2}{q}\right)\pi,$$

which shows that $q > 2$. Together with the definitions of q and γ_0, this implies that $|A|$ satisfies (11), and hence proves (ii). This completes proof of the converse. □

REFERENCES

[B] Beardon, Alan F., *The Geometry of Discrete Groups*, GTM 91, Springer-Verlag, New York, Heidelberg, Berlin, 1983.

[BSt] Beardon, Alan F. and Stephenson, Kenneth, 'The uniformization theorem for circle packings', *Indiana Univ. Math. J.* **39** (1990), 1383–1425.

[F] Ford, L. R., *Automorphic Functons*, 2nd edn, Chelsea, New York, 1951.

[L] Lockwood, E. H., *A Book of Curves*, Cambridge University Press, Cambridge, 1961.

[M] Maskit, B., 'On Poincaré's theorem for fundamental polygons', *Adv. Math.* **7** (1971), 219–230.

[RK] Rothen, F. and Koch, A.-J., 'Phyllotaxis or the properties of spiral lattices. II. Packing of circles along logarithmic spirals', *J. Phys. France* **50** (1989), 1603–1621.

[RS] Rodin, Burt and Sullivan, Dennis, 'The convergence of circle packings to the Riemann mapping', *J. Diff. Geom.* **26** (1987), 349–360.

[Sc] Schramm, Oded, 'Rigidity of infinite (circle) packings', *J. Amer. Math. Soc.* **4** (1991), 127–149.

[T] Thurston, William, 'The geometry and topology of 3-manifolds', preprint, Princeton University Notes.

Authors' addresses:

Alan F. Beardon,
Dept. of Pure Math.
and Math. Statistics,
University of Cambridge,
16 Mill Lane,
Cambridge CB2 1SB,
England.

and

Tomasz Dubejko and Kenneth Stephenson,
Dept. of Mathematics,
University of Tennessee,
Knoxville, TN 37996–1300,
U.S.A.

(Received, October 22, 1991; revised version, September 30, 1992)